Bulletin of the Mineral Research and Exploration

http://bulletin.mta.gov.tr

Active tectonics of western Kosovo: Insights from geomorphic and structural analyses

Alper GÜRBÜZ[a], Astrit SHALA[b], Shemsi MUSTAFA[c] and Aytekin ERTEN[d]

[a] *Niğde Ömer Halisdemir Üniversitesi, Mühendislik Fakültesi, Jeoloji Mühendisliği Bölümü, 51240, Niğde, Türkiye*

[b] *University Isa Boletini Mitrovicë, Faculty of Geosciences, Department of Geology, Str.Ukshin Kovacica, 40000, Mitrovicë, Republic of Kosovo*

[c] *Ministry of Economy, Seismological Network of Kosovo, Geological Survey of Kosovo,10000, Prishtinë, Republic of Kosovo*

[d] *Niğde Ömer Halisdemir Üniversitesi, Fen Bilimleri Enstitüsü, Jeoloji Mühendisliği Anabilim Dalı, 51240, Niğde, Türkiye*

Research Article

Keywords:
Neotectonics, Extensional Tectonics, Shkodër-Pejë Fault Zone, Balkans, Southeast Europe.

ABSTRACT

Kosovo is located in a key position in the central-west part of the Balkans, providing an opportunity to understand the far-field effects of distributed intracontinental deformation caused by the Aegean extension in the south and Adriatic compression in the west. It is also situated along the NE-SW trending Shkodër-Pejë transverse zone, where the Dinarides and Albanides-Hellenides orogenic belts are juxtaposed. While the instrumental seismicity of Kosovo indicates the activity of this fault zone and many others, the active faults in the country were not discussed in detail in the current literature. In this study, we analyzed both the geomorphic and structural features of major mountain front faults in western Kosovo (i.e., Pejë, Istog, Krojmir, and Prizren faults) to reveal the relative assessment of their activities and kinematic characters. Geomorphic and morphometric analyses of all four different mountain fronts studied indicated high activity and tectonic uplift rates of over 0.5 mm/a. On the other hand, according to the collected kinematic data from the observed fault planes, the studied faults are mainly of normal character, representing a dominance of NW-SE-directed extension in western Kosovo, which is most probably caused by the rollback of the subducting slab in the Hellenic trench.

Received Date: 28.09.2022
Accepted Date: 02.01.2023

1. Introduction

Subduction of the African Plate beneath the Anatolian Plate along the Hellenic trench causes a widespread extension that is not limited to the Aegean Sea and affects a large region reaching the central Balkans in the north (Figure 1; e.g., Burchfiel et al., 2006, 2008; Kotzev et al., 2006; Métois et al., 2015). As clearly known, the southern Aegean Sea represents the most rapidly extending region in the world with a rate of 3.5 cm/a (e.g., Taymaz et al., 1990; Reilinger et al., 1997, 2006; McClusky et al., 2000; Le Pichon and Kreemer, 2010). On the other hand, the approximately 800 km long region between the Hellenic trench and the central Balkan Peninsula represents one of the largest intracontinental extensional domains in the world (D'Agostino et al., 2020). In addition to the major role of this extension, the western part of the Balkan Peninsula is also under the effect of compression, which is related to the slow collision between the Adriatic and the Eurasian plates along the Dinarides-Albanides-Hellenides (e.g., Baker et al., 1997; Louvari et al., 2001; Faccenna et al., 2003; Hollenstein et al., 2008; Jouanne et al., 2012; Métois et al., 2015; D'Agostino et al., 2020, 2022). Kosovo

Citation Info: Gürbüz, A., Shala, A., Mustafa, S., Erten, A. 2024. Active tectonics of western Kosovo: insights from geomorphic and structural analyses. Bulletin of the Mineral Research and Exploration 173, 153-173. https://doi.org/10.19111/bulletinofmre.1186708

**Corresponding author: Astrit SHALA, astrit-shala@hotmail.com*

is situated in a key position in the central-west part of the Balkan Peninsula representing the northern part under the influence of the Aegean extensional domain (Figure 1), and provides an opportunity to understand the far-field effects of distributed intracontinental deformation.

The above-mentioned recent framework of the Balkans is based mostly on the geodetic measurements and seismicity recorded in the last decades. However, the geological evolution of the region includes more on geodynamic context effective on today's activity. Kosovo is located where the Dinarides and Albanides-Hellenides orogenic belts are juxtaposed along the NE-SW trending Shkodër-Pejë transverse zone (e.g., Aliaj, 1988; Papa et al., 1991; Muço, 1998; Handy et al., 2019). This structure is known since Aubouin et al., 1970 (i.e., Tranversale de Scutari-Pec) as one of the most important structural elements in the Balkan Peninsula since the Mesozoic. Geological data indicate a right-lateral offset of ophiolitic units along the Shkodër-Pejë transverse zone (Handy et al., 2019). In addition, palaeomagnetic studies demonstrate that this zone represents a separation line in the clockwise rotation of the Albanides-Hellenides at least since the early Neogene with respect to the Dinarides (Figure 1; e.g., Kissel and Laj, 1988; Kissel et al., 1995; Speranza et al., 1995; van Hinsbergen et al., 2005; Bradley et

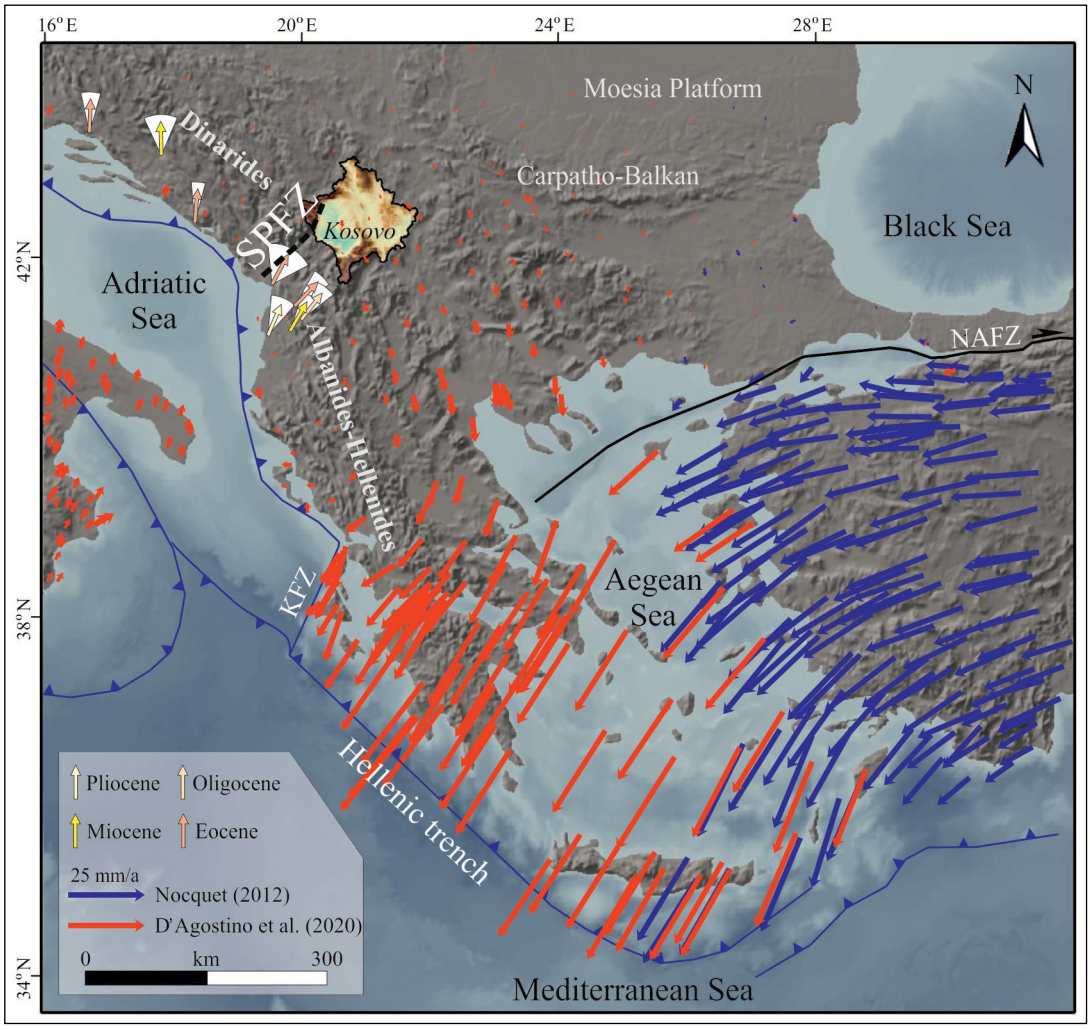

Figure 1- Location map of Kosovo within the active tectonic framework of the Balkan and the Aegean regions showing GPS velocity field with respect to Eurasia (modified from D'Agostino et al., 2020), and the palaeomagnetic declinations for different aged rocks around the Shkodër-Pejë fault zone (SPFZ) relative to African plate (compiled from Kissel et al., 1995 and Speranza et al., 1995 after D'Agostino et al., 2020). NAFZ – North Anatolian fault zone, KFZ - Kephalonia fault zone. For elevation scale of Kosovo please see Figure 3a.

al., 2013). Today, geomorphology, kinematic data, and seismic activity in the region represent that this structure is overprinted by a normal fault zone called the Shkodër-Pejë fault zone (e.g., Muço, 1998; Handy et al., 2015, 2019; Schmitz et al., 2020).

Kosovo includes the eastern part of the Shkodër-Pejë fault zone in its western part (Figure 1). Although the seismicity of the country in the instrumental period indicates the activity of this fault zone and many others (Figure 2a), the active faults in the region were not discussed well in the current literature. In our study, we analysed the geomorphic features of the western part of Kosovo to reveal the relative assessment of major mountain front faults, which are referred to according to the important settlements along the mountain fronts (i.e., Pejë, Istog, Krojmir, and Prizen faults). Because of their bordering position on some major cities of the country, such an approach is also very important in the first step to understanding their seismic risk potential for those cities (i.e., Prizren, Pejë).

2. Geographic and Geological Settings

Kosovo is situated on the central-west Balkan Peninsula at an average altitude of 800 m (Figure 1). Geographically, it is generally addressed within two regions; the eastern part represents a plateau known as the Kosovo Basin, and the western part includes the lowest point (296 m asl), which is bordered by higher mountains with the highest point of the country (2647 m asl), known as Dukagjini Basin (Figure 3a). Eastern Kosovo includes three major drainage basins that flow towards different directions; the Ibër and Morava rivers flow north- and north-eastward into the Danube River towards the Black Sea, and the Lepenci River flows into the Vardar River towards the Aegean Sea in the south (Figure 3b). Almost all of western Kosovo is drained by the Drini i Bardhë River flowing into the Adriatic Sea to the west. While the climate is predominantly continental with cold winters and warm summers, the eastern and western regions represent some differences because of topographic characteristics. Eastern Kosovo represents a more continental climate with a precipitation ratio of 600 mm/a, whereas western Kosovo is influenced by the air masses crossing the Adriatic Sea resulting in higher precipitation ratios (e.g., Elezaj and Kodra, 2007).

Geologically, Kosovo is positioned where the Dinarides, Albanides-Hellenides, and Carpatho-Balkan units juxtaposed (e.g., Elezaj, 2009) (Figure 1). Thus, there are various sedimentary, magmatic,

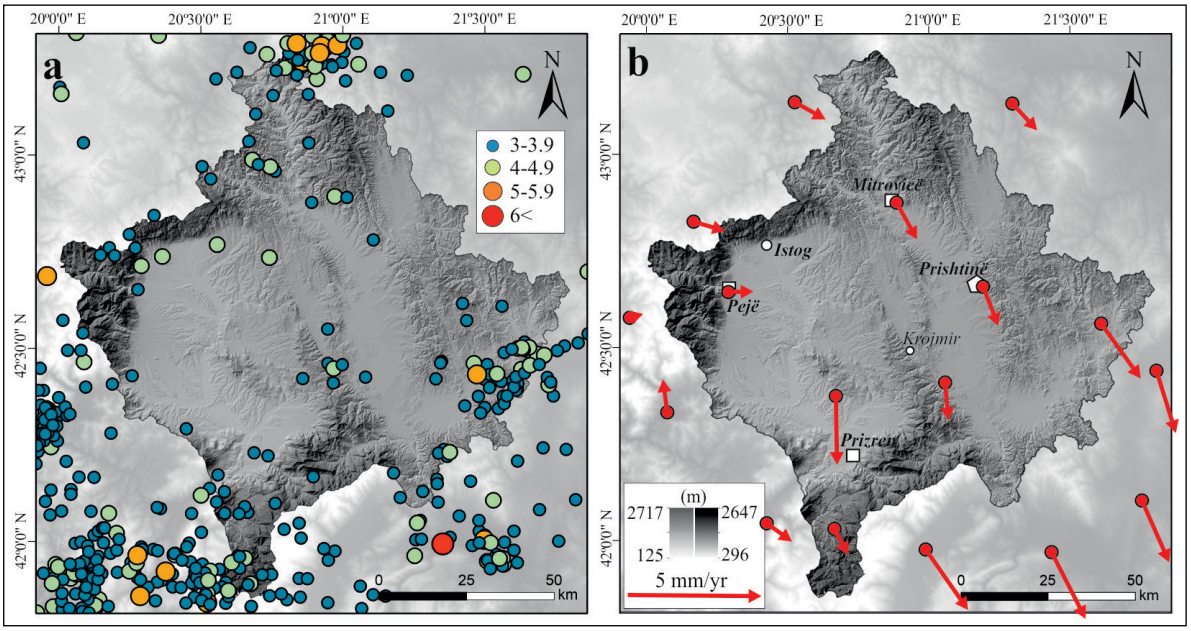

Figure 2- a) Seismicity of Kosovo between 1900-2020 from the USGS earthquake catalogue and b) GPS velocity field with respect to Eurasia from D'Agostino et al. (2020). Darker colour shade is for Kosovo from the topography digitized from 1:25.000 scaled maps in our study, and lighter shade is for the surrounding topography from SRTM.

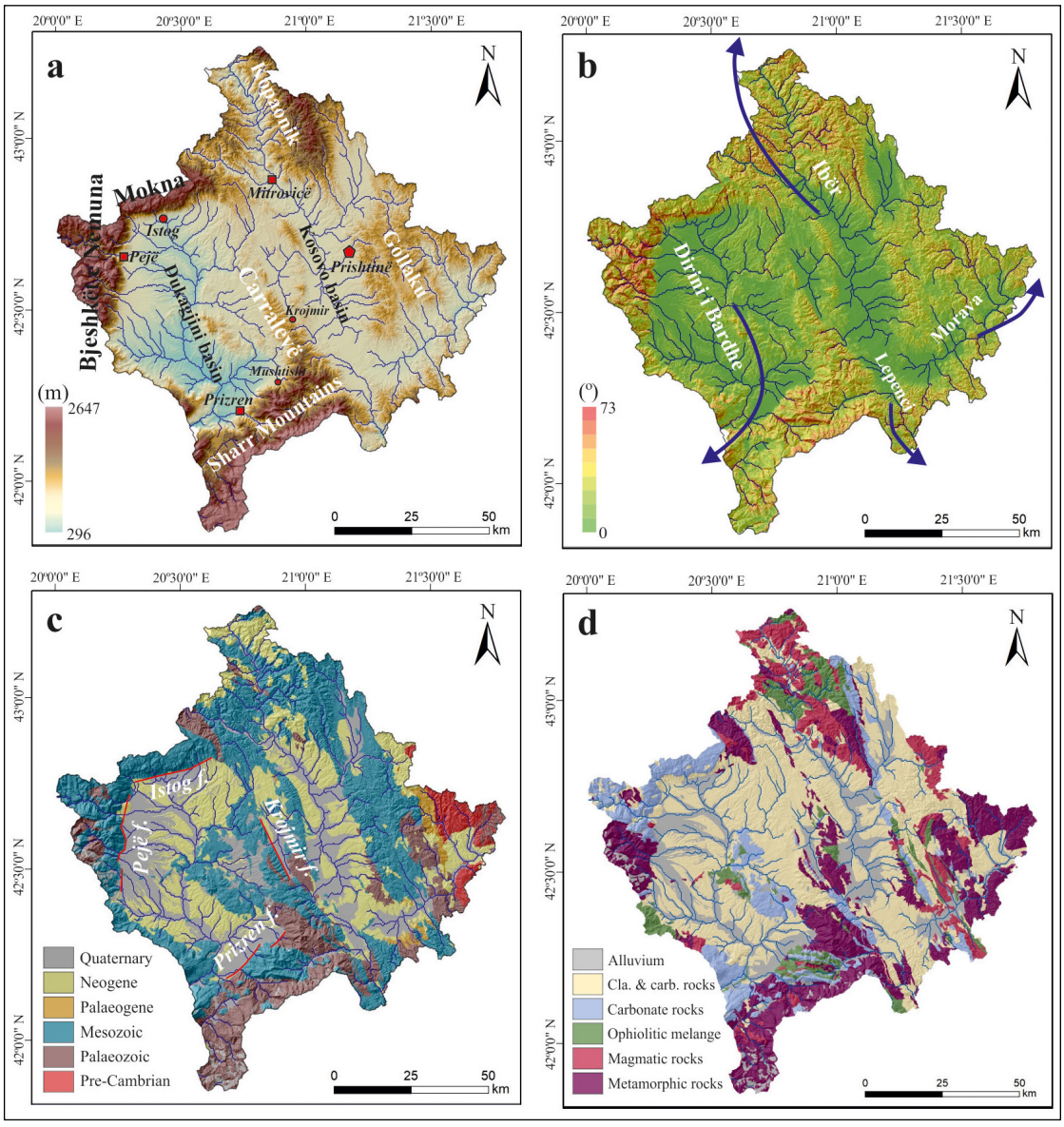

Figure 3- a) Physiographic image of Kosovo as digitized from 1:25.000 scaled topographic maps showing major ranges and basins, b) slope map of Kosovo and major drainage systems with their flowing directions, c) geological age map of Kosovo and the studied mountain front faults in our study (red lines; f – fault), d) lithology map of Kosovo. Both the age and lithology maps (c and d) are derived from KPMM (2006) which is based on Osnovna Geološko Karta SFRJ 1:100,000 – Geološki Institut, Beograd (1970-1984).

and metamorphic formations ranging from Pre-Cambrian to Quaternary complicated with folded and faulted architectures (Figures 3c and 3d). The oldest geologic units are mostly exposed to the mountainous regions surrounding the Kosovo and Dukagjini basins. While the Pre-Cambrian metamorphic rocks outcrop in the easternmost part of Kosovo, the Palaeozoic metamorphic and magmatic rocks are distributed whole of the country, but majorly exposed in the south, at the Sharr Mountains. On the other hand, the Mesozoic units are represented by a variety of lithology including ophiolitic melange, metamorphic, magmatic, and sedimentary rocks (mostly carbonates), and distributed widely in the country. The Neogene units consist of sedimentary and volcanic rocks that are particularly important in the geological evolution of Kosovo, because of their spatial distributions covering most of the Kosovo and Dukagjini basins, which are majorly delimited by the neotectonic structures (e.g., Elezaj, 2009, 2012). The Quaternary units are also

very important because of their positions controlled by recent drainage patterns and mainly by mountain front faults, which are the focus point of our study.

3. Methods

3.1. Geomorphic Analyses

In this study, we constructed a digital elevation model (DEM) of Kosovo with 10 m resolution by digitizing 1:25000 scale topographic maps. To quantify the geomorphic responses to active tectonics we used indices including mountain front sinuosity (S_{mf}), basin shape ratio (B_s), asymmetry factor (A_f), valley floor width-to-height (V_f), hypsometric curve and integral (HI), and normalized steepness index (k_{sn}). To select the ideal mountain fronts and related uplifted areas for analyses, we derived Red Relief Image Map of Kosovo providing detailed terrain surface information from our 10 m resolution DEM. After selecting four mountain fronts that correspond to neotectonic structures referred to as Pejë, Istog, Krojmir, and Prizren faults, we analysed 40 drainage basins on the mountains and ridges related to the mentioned mountain fronts and calculated the relative tectonic activity classes of each mountain front fault geomorphometrically. Lastly, we visited these locations to make field observations for interpreting our morphometric results reliable.

3.1.1. Red Relief Image Map

Red relief image map (RRIM) build by the derivation of negative openness, positive openness, and slope images obtained from the DEM, and is very useful in active tectonics (e.g., Yao et al., 2019). While negative openness represents concavity of the terrain surface by highlighting depressions, positive openness represents convexity by highlighting ridges and crests (e.g., Yokoyama et al., 2002; Ulusoy et al., 2020). Chiba et al. (2008) suggested a parameter based on

$$I = (O_p - O_n)/2 \quad (1)$$

where O_p is positive and O_n is negative openness that eliminates incident light direction dependency and expresses both concavity and convexity. RRIM is based on this parameter shown in a greyscale overlain by a red colour-scale slope image (Chiba et al., 2008; Figure 4).

3.1.2. Mountain Front Sinuosity

The mountain front sinuosity index (S_{mf}), which reflects the balance between tectonic activity and erosion affecting a mountain front, is defined as

$$S_{mf} = L_{mf}/L_s \quad (2)$$

where L_{mf} is the length of the mountain-piedmont junction and L_s is the straight-line length of the mountain front (Bull and McFadden, 1977). While values close to 1.0 reflect less sinuous, relatively straight mountain fronts related to high tectonic activity, higher values represent high sinuosity related to the dominance of erosional processes over tectonic activity and reflect relative quiescent (e.g. Keller, 1986; Silva et al., 2003). In this study, we calculated S_{mf} index for 4 mountain fronts.

3.1.3. Basin Shape Ratio

The drainage basin shape index (B_s) of streams crossing mountain fronts reflects base-level changes arising from relative tectonic uplift and is defined by an elongation ratio expressed as

$$B_s = B_l / B_w \quad (3)$$

where B_l is the length and B_w is the width of the basin (Ramirez-Herrara, 1998). High values are associated with elongated basins indicating relatively high tectonic activity and rapidly uplifted mountain fronts, whereas low values represent more circular basins related to low tectonic activity (e.g. Ramirez-Herrara, 1998; El Hamdouni et al., 2008). This index was calculated for the 40 drainage basins of streams on the studied ranges in the western half of Kosovo in order to identify the elongated basins revealing rapid uplift.

3.1.4. Asymmetry Factor

The drainage basin asymmetry factor (A_f), which evaluates the tilting of the drainage basin related to tectonic activity, is calculated through

$$A_f = (A_r/A_t)\ 100 \quad (4)$$

where A_r is the area of the basin to the right of the trunk stream while facing downstream, and A_t is the total area of the drainage basin (Hare and Gardner, 1985). If the value is close to 50, the basin evaluated has less

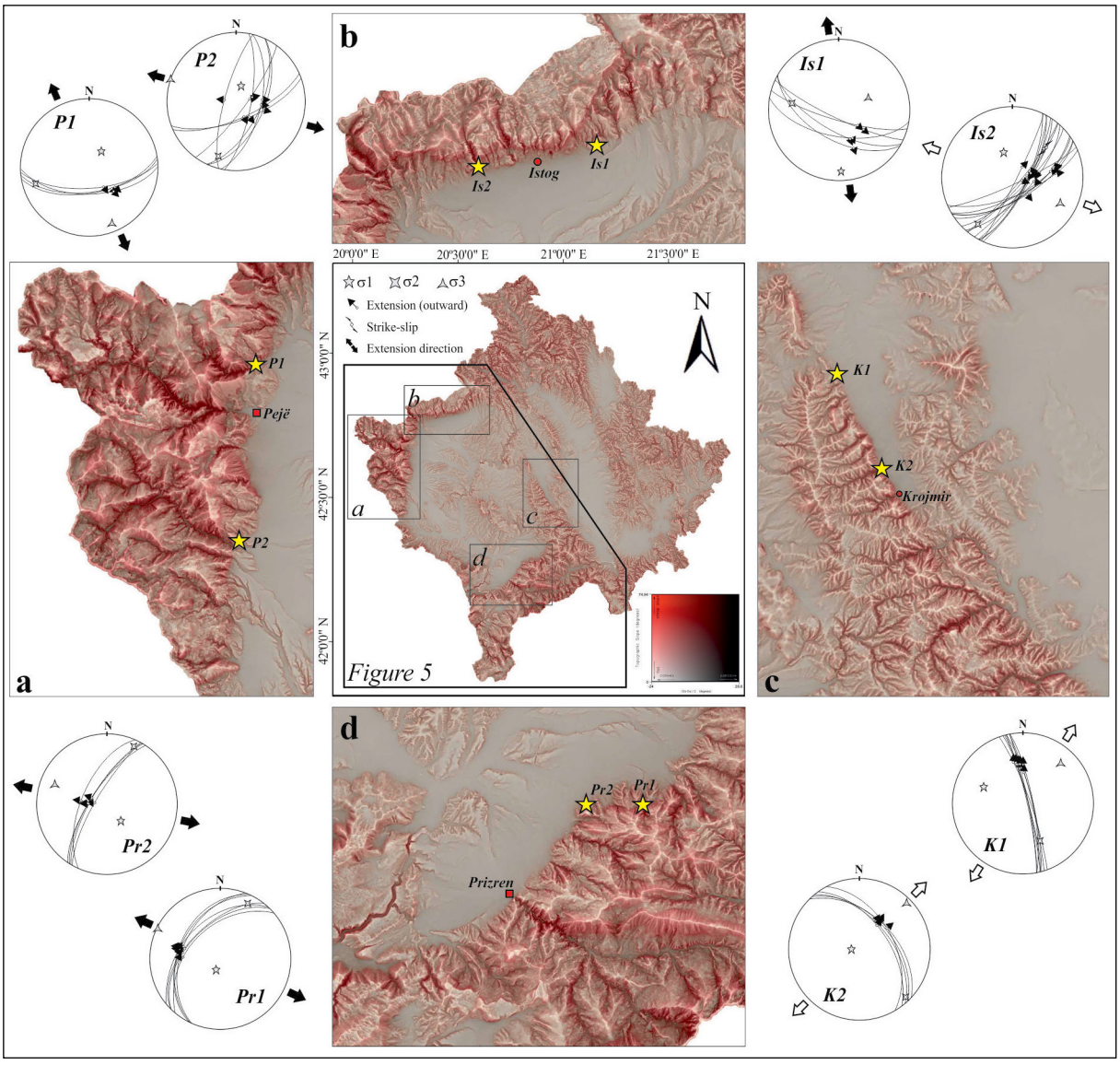

Figure 4- The Red Relief Image Map (RRIM) of Kosovo represents the geomorphic traces of studied mountain front faults and cyclographical traces, stress orientations and striations collected from the faults (Lower hemisphere equal area projection). Yellow stars with P – Pejë, Is – Istog, K – Krojmir and Pr – Prizren indicate measured fault plane locations.

or no tilting and is stable, whereas values far below or far above 50 represent the drainage basin is under the effect of tectonic tilting and/or differential erosion of lithology and is unstable (e.g. Keller and Pinter, 2002; El Hamdouni et al., 2008). In our study, the asymmetry factor is calculated for 40 drainage basins on four ridges to consider any tilting process related to active tectonic deformation and/or lithological control.

3.1.5. Valley Floor Width-to-Height Ratio

The valley floor width-to-height ratio (V_f) of streams differentiates the wide floored valleys and narrow floored valleys relative to their wall heights and is computed by

$$V_f = 2V_{fw} / [(E_{ld} - E_{sc}) + (E_{rd} - E_{sc})] \quad (5)$$

where V_{fw} is the width of the valley floor, E_{ld} and E_{rd} are the elevations of the left and right sides of the valley, and E_{sc} is the elevation of the valley floor (Bull and McFadden, 1977). While V_f values lower than 1.0 represent V-shaped valleys associated with high incision rates, values higher than 1.0 indicate U-shaped valleys related to high lateral erosion (Bull and McFadden, 1977; Silva et al., 2003). The incision

is generally related to uplift, thus the index represents tectonic activity (El Hamdouni et al., 2008). Because of V_f values can considerably change related to their positions along the valley (Ramirez-Herrera, 1998), to make meaningful comparisons among different valleys values are often calculated at a given distance from the stream mouth (Silva et al., 2003; Cheng et al., 2018). In our study, positions of the V_f cross-sections have been chosen with a distance of 1 km from each of the 40 stream mouths.

3.1.6. Hypsometry

Hypsometry is an important approach for active tectonics (e.g. Keller and Pinter, 2002) and is highly sensitive to continued topographic evolution (e.g. Harlin, 1978; Mayer, 1990). The hypsometric curves are constructed by plotting the proportion of total basin elevation versus the proportion of total basin area, thus expressing the volume of a basin that has not been eroded (e.g. El Hamdouni et al., 2008). The hypsometric integral (*HI*) index describes the distribution of elevation of a given area of a landscape, particularly for drainage basins, (Strahler, 1952) and is calculated as

$$HI = (H_{mean}-H_{min})/(H_{max}-H_{min}) \quad (6)$$

where H_{mean} is the mean, H_{max} is the maximum, and H_{min} is the minimum elevations (e.g. Pike and Wilson, 1971; Mayer, 1990; Keller and Pinter, 2002). While high values generally indicate low eroded material and a young landscape probably produced by active tectonics, low values majorly represent high erosion rates and less tectonic uplift (e.g. El Hamdouni et al., 2008). In our study, we computed the hypsometric curves and integrals for 40 drainage basins to discuss the roles of constructive tectonic and destructive erosive forces.

3.1.7. Normalized Channel Steepness Index

The normalized channel steepness index (k_{sn}) is a convenient approach for active ranges to Figure out a relative assessment of tectonic uplift rates (e.g., Wobus et al., 2006; Dibiase et al., 2010; Kirby and Whipple, 2012). Because the channel steepness index is sensitive to changes in uplift rates, lithology and climate at steady-state, while the concavity of most stream channels on mountains has uniform concavity independent from the uplift rates (Snyder et al., 2000; Whipple, 2004; Kirby and Whipple, 2012). Normalization of this index is useful to compare streams and catchments of different drainage areas through their profile morphology (Sukhishvili et al., 2021). Streams on both bedrock and alluvial rivers have typically concave profiles that can be described by an empirical power law relationship:

$$k_{sn} = SA^{\theta} \quad (7)$$

Where S is the slope, A is the drainage area and θ is the channel concavity index (Flint, 1974; Sukhishvili et al., 2021). Practically, values between 0.4 and 0.5 work well for most mountain streams as a reference concavity (θ_{ref}) (Kirby and Whipple, 2012); thus, we used 0.45 for θ_{ref} in this study as generally accepted (e.g., Kirby and Whipple, 2012; Han et al., 2017; Kothyari et al., 2020). We mapped k_{sn} values of the fluvial systems in western Kosovo based on construction through the kernel density values, which indicate how well features are clustered Figure 11(e.g., Sun and Mann, 2021).

3.2. Structural Analyses

In the field, a total of 58 fault slip data were collected and analysed, which are considered as the younger movements for the studied mountain front faults (12 data from 2 locations on the Pejë, 21 data from 2 locations on the Istog, 13 data from 2 locations on the Krojmir and 12 data from 2 locations on the Prizren mountain fronts). We used WinTensor 5.9.2 (Delvaux and Sperner, 2003) for stress analyses.

4. Results

4.1. Pejë Fault

NNE-SSW-directed Pejë fault bounds the Dukagjini Basin from the west with a length of ~35 km. The fault defines the front of Bjeshkët e Nemuna mountains with a sharp slope break (Figures 3b, 3c, and 4), which consists of Palaeozoic and Mesozoic metamorphic and Mesozoic carbonate rocks (Figures 3c and 3d), and represents an S_{mf} value of 1.26 (Table 1). Ten drainage basins that analyzed related to the Pejë fault have V_f values in the range of 0.03 and 0.29, values of B_s ranging from 1.55 to 5.29, A_f values between 29.66 and 76.33, and *HI* values

ranging from 0.41 to 0.58 (Figure 5; Table 1). The hypsometric curves represent a majorly mature to a bit young stage, approximately from south to north (Figure 11). The k_{sn} analyses of the streams on the Bjeshkët e Nemuna Mountains represent high values, particularly in the northern part where the lithology is mainly represented by carbonate sedimentary rocks (Figure 6). The geomorphology of this mountain front actually supports these morphometric results with clear geomorphic proofs of activity such as trapezoidal to triangular facets and well-developed piedmont and alluvial fan deposits (Figure 7). According to the kinematic data collected from the field in two locations, the eastward dipping normal fault indicates WNW-ESE-directed extension (Figures 4 and 7; Table 2). While we could not observe a direct contact of the fault plane with Quaternary deposits, the strikes of the fault planes are compatible with the ~ N-S orientation of the fault (Figure 4).

4.2. Istog Fault

The E-W trending and southward dipping Istog fault bounds the Mokna Mountains from the south along a ~25 km long front that corresponds to the

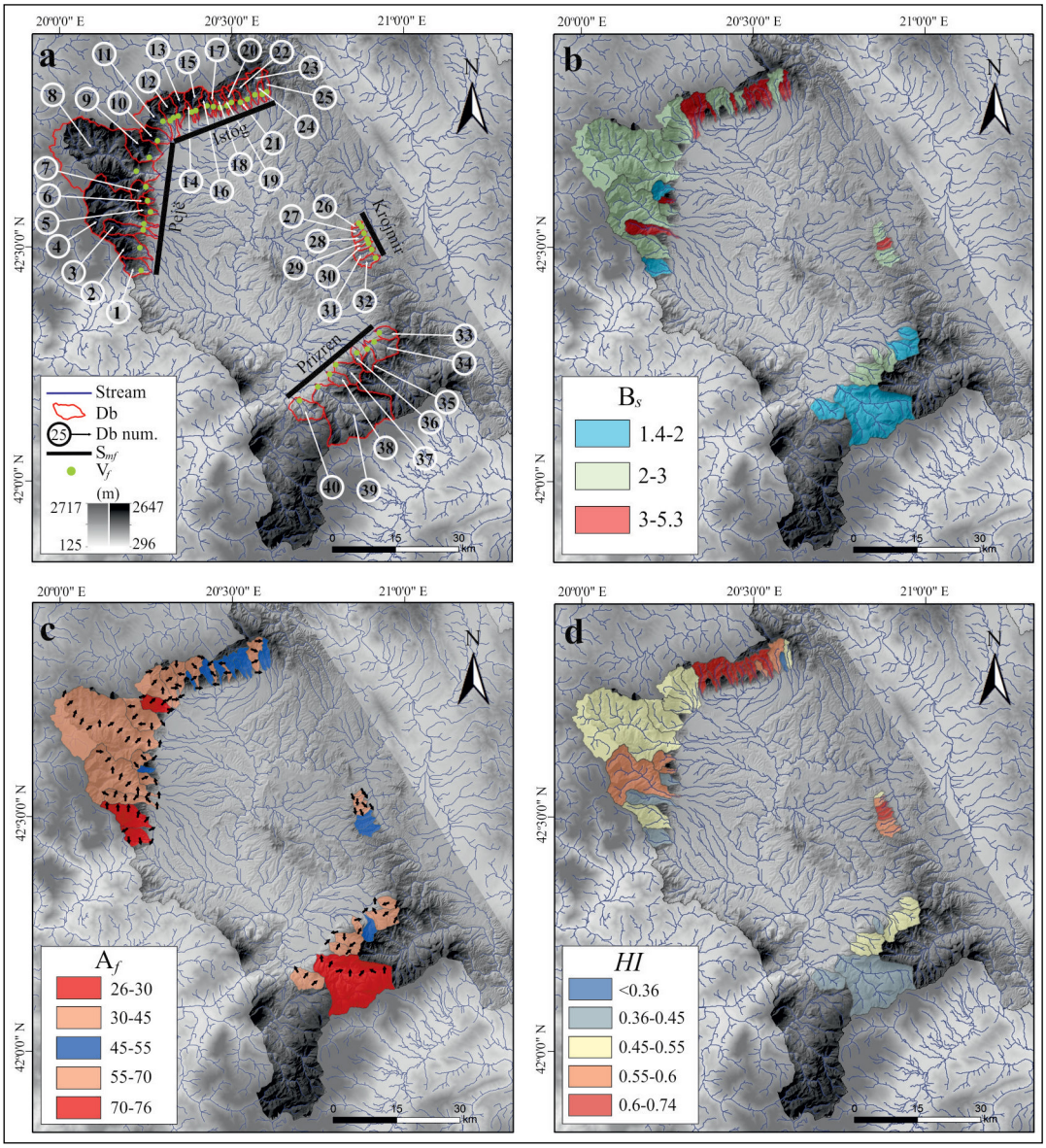

Figure 5- a) Index map for the locations of calculated S_{mf}, V_f and other indices for the drainage basins (Db – drainage basin), b) B_s, c) A_f, and d) *HI* values calculated for these drainage basins along the studied parts of the mountain front faults.

Table 1- Results of the morphometric indices used for the studied four mountain front faults in western Kosovo.

Mountain front fault	S_{mf}	Drainage basin no.	V_f	B_s	A_f	HI
Pejë	1.26	1	0.05	1.61	29.66	0.41
		2	0.29	2.21	75.35	0.47
		3	0.12	5.29	68.09	0.45
		4	0.06	2.57	68.78	0.56
		5	0.1	2.14	55.62	0.42
		6	0.1	3.73	47.58	0.55
		7	0.06	1.55	38.38	0.58
		8	0.03	2.3	55.89	0.54
		9	0.03	2.27	41.38	0.55
		10	0.05	2.14	76.33	0.54
Istog	1.06	11	0.1	2.29	65.53	0.53
		12	0.14	3.87	57.86	0.51
		13	0.15	4.1	37.51	0.66
		14	0.13	5.31	52.72	0.63
		15	0.08	2.93	58.73	0.72
		16	0.08	2.95	53.06	0.65
		17	0.17	4.79	41.22	0.65
		18	0.39	2.97	53.14	0.73
		19	0.1	4.84	40.26	0.66
		20	0.05	4.27	46.23	0.74
		21	0.15	4.83	48.25	0.55
		22	0.25	3.08	47.19	0.6
		23	0.09	2.86	62.93	0.56
		24	0.15	4.13	46.83	0.36
		25	0.31	4.96	47.52	0.46
Krojmir	1.11	26	0.22	2.72	34.4	0.5
		27	0.16	2.14	36.47	0.58
		28	0.17	2.64	40.53	0.6
		29	0.09	3.2	42.92	0.61
		30	0.16	4.16	49.15	0.61
		31	0.13	2.64	47.62	0.59
		32	0.08	2.09	46.63	0.59
Prizren	1.28	33	0.17	1.9	63.06	0.47
		34	0.18	1.58	33.77	0.52
		35	0.16	2.24	49.52	0.51
		36	0.15	2.03	30.1	0.44
		37	0.12	2.19	56.76	0.52
		38	0.12	2.23	40.13	0.47
		39	0.14	1.4	26.03	0.42
		40	0.29	1.55	40.12	0.45

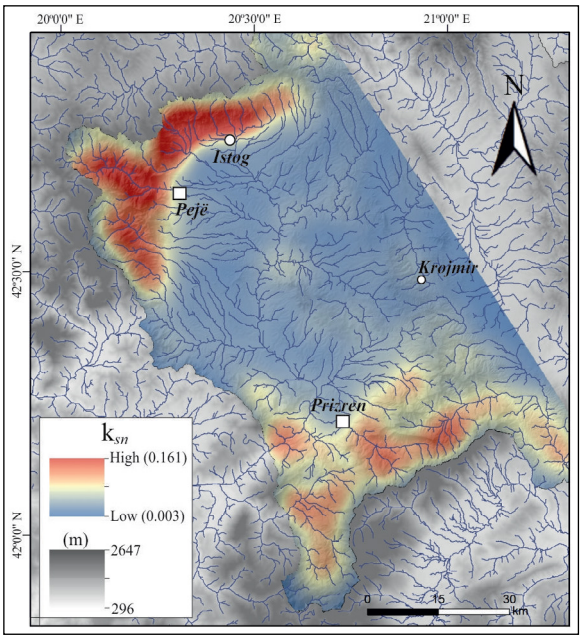

Figure 6- The k_{sn} map of western Kosovo constructed through the kernel density values.

northern margin of the Dukagjini Basin (Figures 3b, 3c, and 4). Except for a little area of metamorphic and magmatic rocks to the easternmost part of the mountain, the main lithology cut by the Istog fault is Mesozoic carbonate rocks (Figures 3c and 3d). The mountain front has a S_{mf} value of 1.06, which is the lowest S_{mf} value among the studied four mountain fronts (Table 1). Among the studied mountain front faults, the Istog fault was studied through the highest number of drainage basins. Fifteen drainage basins have the V_f values in the range of 0.05 and 0.39, values of B_s ranging from 2.29 to 5.31, A_f values between 37.51 and 65.53, and hypsometric integral values ranging from 0.36 to 0.74 (Figure 5; Table 1). Almost whole of the drainage basins on the Mokna Mountains represents the youthful stage according to hypsometric curves (Figure 11). According to the k_{sn} analyses, while the values decrease towards the east along the mountains, this region represents the highest k_{sn} values in western Kosovo (Figure 6). In addition to these, morphometric proofs of high activity level, geomorphic observations of a steep scarp with trapezoidal and triangular facets, deeply incised valleys, and aligned water springs along the Istog fault also indicate the rapid uplift/high activity (Figure 8). In the field, we measured fault slip data at two locations on the eastern and western parts of the Istog fault (Table 2). Our data represent normal faulting developed as a result of NW-SE-directed extension in the region (Figure 4). Particularly to the western part of the fault, the brecciated fault plane with contact in Quaternary deposits including normal drag fold represents the fault character and its activity in the Quaternary period (Figure 8).

4.3. Krojmir Fault

NW-SE trending and eastward dipping Krojmir fault delimits the Carralevë Mountains from the east with a steep slope, which is located in central Kosovo, that separates the Dukagjini basin from the Kosovo basin (Figures 3b, 3c and 4). Among the heights delimited by the studied faults, the Carralevë Mountains represent the lowest topography with a maximum height of 1177 m. The main lithology

Table 2- Fault slip data measured along the studied mountain fronts in western Kosovo (σ1, σ2 and σ3: Trend and plunge of principal stress axes; R: Stress ratio).

Mountain front fault	Location	Coordinate		σ1	σ2	σ3	R	N	Age/Lithology
		North	East						
Pejë	P1	42° 42' 19"	20° 17' 28"	037/67	253/19	159/13	0.49	4	Mesozoic / limestone
	P2	42° 33' 22"	20° 16' 15"	018/72	198/18	288/00	0.38	8	Mesozoic / metaclastics
Istog	Is1	42° 47' 41"	20° 31' 49"	068/53	278/33	178/14	0.5	5	Mesozoic / metacarbonates
	Is2	42° 46' 42"	20° 24' 15"	341/59	217/18	118/23	0.53	16	Mesozoic / limestone and volcanosedimentary
Krojmir	K1	42° 34' 8"	20° 52' 16"	293/40	155/42	043/23	0.5	8	Mesozoic / serpentinite
	K2	42° 30' 5"	20° 54' 58"	267/80	136/06	046/07	0.49	5	Mesozoic / serpentinite
Prizren	Pr1	42° 16' 34"	20° 51' 58"	201/76	026/14	296/01	0.57	7	Mesozoic/ limestone
	Pr2	42° 16' 41"	20° 48' 49"	144/69	030/09	297/18	0.5	5	Mesozoic / peridotite

Figure 7- Field photos from the Pejë mountain front fault; a) slope break on the topography to the south of Pejë. b) triangular facets to the southwest of Deçan, c), d) and e) fault plane and kinematic indicators observed in P1 (please see Figure 4 for the location). In (e) the right-lateral slip represents older movement and it is overprinted by normal slip with left-lateral component representing the younger movement on the fault plane.

includes Palaeozoic metamorphic rocks and Mesozoic volcanoclastic rocks, serpantinites, carbonate, and clastic sedimentary rocks (Figures 3c and 3d) The Krojmir fault extends more than 30 km; however, actually, the slope break delimiting the studied part of the mountainous topography corresponds to a length of ~15 km. The mountain front created by the Krojmir fault has a S_{mf} value of 1.11, which is the second lowest value after the Istog fault (Table 1). Only seven drainage basins corresponding to the southern half of the studied mountain front were analysed morphometrically. The V_f values range from 0.08 and 0.22, B_s values are between 2.09 and 4.16, A_f values range between 34.40 and 49.15, and *HI* values range from 0.5 to 0.61 (Figure 5; Table 1). Hypsometric curves of the drainage basins on the

Figure 8- Field photos from the Istog mountain front fault; a) slope break on the topography, b) faulted topography and deeply incised valley representing rapid tectonic uplift, c) Istog water spring is one of the most important water sources of Kosovo, which is positioned on the Istog fault, d) fault plane observed in Is2 (please see Figure 4 for the location). Please note the normal drag fold (hanging-wall syncline) in Quaternary deposits associated with friction during the uplift of the footwall.

Carralevë Mountains dominantly represent a young stage (Figure 11). However, the streams on this part of the mountains have the lowest k_{sn} values among the studied ranges, because of the low strength of clastic rocks. On the other hand, geomorphological field observations along the fault support the general geomorphometric results indicating its activity with well-developed triangular facets along a straight line (Figure 9). Among all the mountain front faults studied in this study, with respect to its clear imprint on the topography, finding a reliable young fault plane is hard along the Krojmir fault because of highly deformed older lithological units. However, on the northern and southern parts of the fault, the kinematic data collected from two locations on serpentinites indicate both oblique-slip and normal faulting with NE-SW directed extension (Figures 4 and 9; Table 2).

4.4. Prizren Fault

NE-SW trending and NW-wards dipping Prizren fault bounds the Dukagjini Basin from the south with a ~30 km length (Figures 3b, 3c, and 4). This line also coincides with the northern front of the Sharr Mountains, which is one of the major ranges in the region with a maximum height of 2651 m (Figures 3a and 4). The Sharr Mountains consist of a variety of lithology among the other studied mountains including Palaeozoic metamorphic rocks and Mesozoic magmatic, metamorphic, ophiolitic melange, and carbonate rocks (Figures 3c and 3d). S_{mf} value for the Sharr Mountains along the Prizren fault is 1.28, which is the lowest among the studied faults (Table 1). Geomorphometric indices applied for eight drainage basins on the range represent V_f values ranging from 0.12 to 0.29, Bs values between 1.4 and 2.24, A_f values ranging from 26.3 to 63.06, and hypsometric integral values between 0.42 and 0.52 (Figure 5; Table 1). Hypsometric curves of the drainage basins flowing towards the Dukagjini Basin on the Sharr Mountains majorly represent the mature stage (Figure 11). The streams represent the second lowest k_{sn} values among the studied ranges. Triangular

Figure 9- Field photos from the Krojmir mountain front fault; a) slope break on the topography, b), c) triangular facets. Fault planes in d) K1 and e) K2 locations to the north and south of the mountain front fault, respectively. Please see Figure 4 for the locations.

facets and alluvial fans are aligned along the Prizren fault (Figure 10). In the field, we observed a normal fault plane coincides with the topographic trace of the Prizren fault towards east (Figures 10c and 10d). Kinematic data on the fault plane represent NW-SE-directed extension (Pr1; Figure 4, Table 2).

5. Discussion

5.1. Assessment of Relative Activity and Implications on the Seismicity of Western Kosovo

Tectonic activity classification based on the correlation of S_{mf} and V_f indices is helpful to evaluate the relative activity of mountain front faults (e.g., Bull and McFadden, 1977; Rockwell et al., 1985; Silva et al., 2003). According to our results, all of the studied faults are within Class 1 representing high activity, which also indicates uplift rates of >0.5 mm/a (Figure 12). These results are also coherent with the results of individual other indices, such as with B_s and HI (Table 1; Figure 5d), pointing out the higher activities of the Istog and Krojmir faults. These are followed by the activity levels of Pejë and Prizren faults, respectively. According to the A_f values, the Istog and Krojmir faults represent the more neutral character, while the drainage basins along the Pejë and Prizren mountain

Figure 10- Field photos from the Prizren mountain front fault; a) triangular facets, b) slope break on the topography. c, d) Observed normal fault plane in Pr1. Please see Figure 4 for the location.

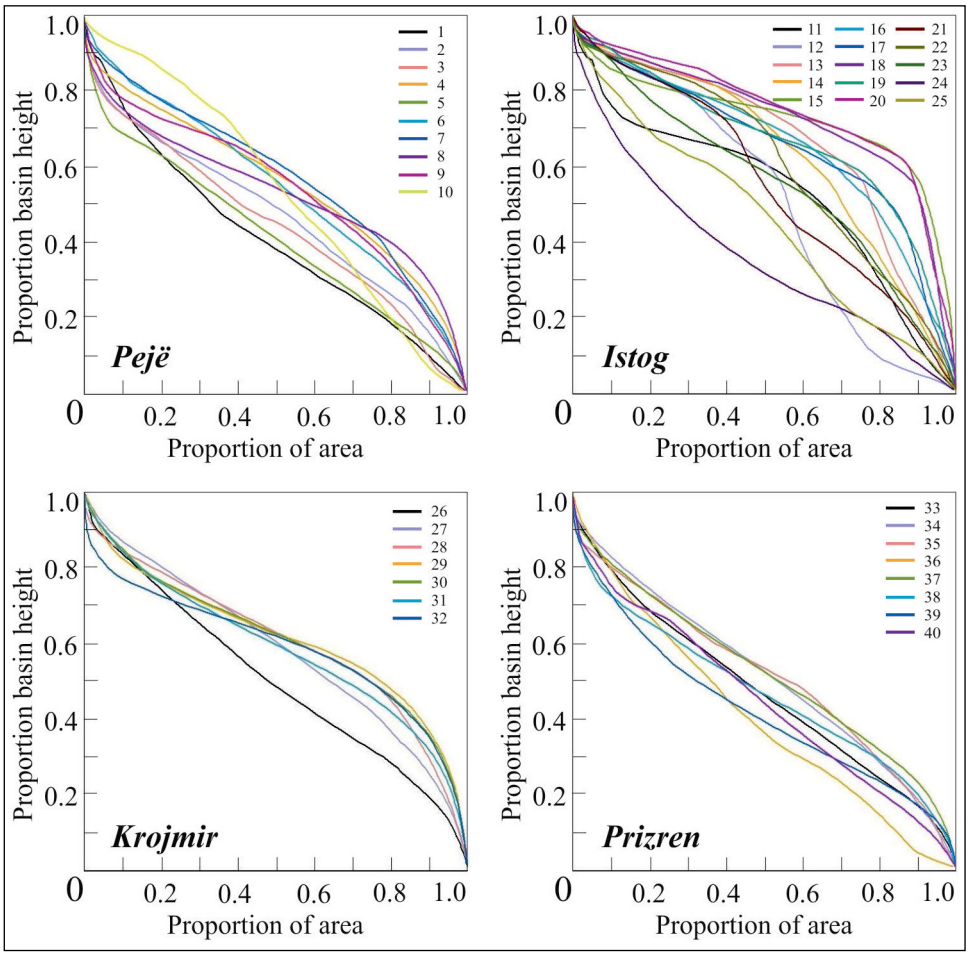

Figure 11- Hypsometric curves of the drainage basins on the studied mountain front faults.

front faults have prominent asymmetries, most probably because of weaker lithological features on the last two mountain fronts consisting of ophiolitic melange and metamorphic rocks. On the other hand, the k_{sn} values represent the higher activity along the Pejë and Istog normal faults clearly than the Prizren and Krojmir faults. D'Agostini et al. (2022) suggested that the Istog fault has no significant evidence of recent activity, and the Pejë fault is more active than the Istog based on their observations. However, according to our aforementioned geomorphometric results, the Istog fault represents higher activity. Among the studied mountain front faults, while all of them have direct contact majorly with the Quaternary deposits (Figure 3c) showing their probable activities in this period, observed normal drag fold within the colluvial deposits on the Istog fault represents the effect of normal faulting on the Quaternary units (Figure 8d). Evaluating their geomorphic, morphometric and structural features together, the studied Pejë, Istog, Krojmir, and Prizren normal faults are active faults that can create earthquakes with magnitudes 6.4 to 6.8, according to the empirical relationship of Wells and Coppersmith (1994), if they ruptured along their mountain front total lengths.

Today, Kosovo exhibits moderate seismicity (Sulstarova and Aliaj, 2001; Elezaj, 2002; Muço et al., 2012). However, there are important historical records in the country (Mustafa et al., 2020). Among them, there are two historical earthquakes corresponding to the studied faults in our study with magnitudes 6.6 (1456 earthquake) at Prizren and 6.0 (1662 earthquake) at Pejë (Orana et al., 1985; Muço et al., 2012; Mustafa, 2016). On the other hand, whereas some important earthquakes recorded in the instrumental period with a magnitude over 5 within the boundaries of the country (24/4/2002 earthquake at Gjilan, SE of Kosovo),

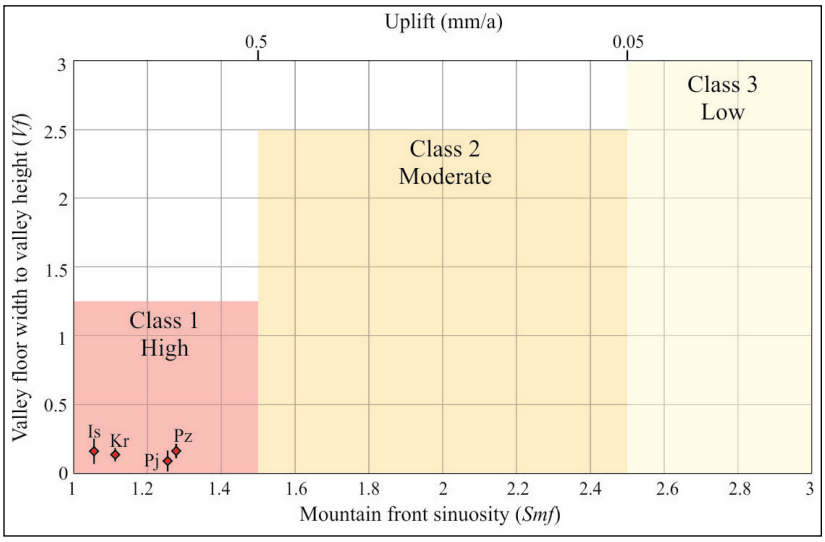

Figure 12- Inferred activity classes of the studied mountain front faults in western Kosovo based on the plot of S_{mf} vs V_f after Bull and McFadden (1977), and inferred uplift rates (U) after Rockwell et al. (1985).

among the studied faults, the Istog and Krojmir faults have records reaching over the magnitude 4.5 (Figure 2a). Both the historical and instrumental seismicity recorded in western Kosovo also support our aforementioned results and implications, which can be summarized as a high activity class for all the studied mountain front faults.

5.2. Implications on the Regional Tectonics

At the Dinarides-Hellenides belt transition, Neogene tectonics, and associated fault systems are regulated by mechanisms induced by the Hellenic slab roll-back (Figure 1a) (e.g., Handy et al., 2019). As aforementioned, the Shkodër-Pejë transverse zone was originally a transform fault as evidenced by the 100 km displacement of the ophiolitic melanges to the north and south of the fault; however, today, it represents normal fault character as evidenced by the kinematic data collected majorly in northern Albania and southern Montenegro, enabling the rotation movement of the Albanides-Hellenides with respect to Dinarides (e.g., Handy et al., 2015, 2019; Biermans et al., 2019). According to our field observations, fault slip data on the planes of the Pejë fault, which corresponds to the eastern extension of the Shkodër-Pejë fault zone (e.g., Handy et al., 2015, 2019), supported the normal faulting in the region (e.g., D'Agostino et al., 2022). On the other hand, while our geomorphic analyses along the four mountain fronts in western Kosovo represented high activity, the k_{sn} values clearly shone out the higher activity of Pejë and Istog faults and supporting their probable continuity as part of an important fault zone (i.e., Shkodër-Pejë fault zone), as suggested by some authors (e.g., Schmid et al., 2020). The Prizren fault also shows normal fault character as evidenced by the kinematic data. The Krojmir fault exhibits fault slip data indicating oblique and normal character. In such a scene, while the Pejë, Istog and Prizren faults represent NW-SE-directed extension in the region, the Krojmir fault has kinematic indicators supporting NE-SW-oriented extension.

Such an extensional tectonic regime has been known for the south Balkans since the Palaeogene, however, the recent phase of extension in the region started just after a short post-Palaeogene shortening, in the early Neogene (e.g., Burchfiel et al., 2000, 2006, 2008; Dumurdzanov et al., 2005). Since that time, the Albanides-Hellenides has rotated clockwise with respect to Dinarides and Africa (Figure 1; Kissel et al., 1995; Speranze et al., 1995; van Hinsbergen et al., 2005; Handy et al., 2019; D'Agostino et al., 2020) because of pulling along the Hellenic trench and tearing of the underlying Adriatic plate (e.g., Handy et al., 2019). On the other hand, there is a contraction to the west between the Adriatic and Eurasian plates,

which is associated with great earthquakes responsible for many casualties and economic losses (e.g., 1979 Montenegro earthquake - Mw=7.1, and 2019 Albania earthquake - Mw=6.4; Benetatos and Kiratzi, 2006; Papadopoulos et al., 2020). However, this NE-SW trending contraction is replaced by an extension in the hinterland due to rollback (e.g., D'Agostino et al., 2008, 2020; Nocquet, 2012; Biermanns et al., 2022). Because of the effects of extension caused by the rollback of subducting slabs in the Aegean and Adriatic seas, and the clockwise rotation of the Albanides-Hellenides to the south of Shkodër-Pejë fault zone (e.g., Jouanne et al., 2012; Faccenna et al., 2014; Handy et al., 2015; Biermanns et al., 2022), western Kosovo has mountain fronts controlled by majorly normal faults representing a dominance NW-SE-directed extension in this part of Balkans, coherent with the GPS data (Figures 1 and 2b).

6. Conclusions

The topographic features of the country represent faulted mountain fronts with clear geomorphic indicators of activity, particularly in western Kosovo delimiting the Dukagjini Basin. In this study, to understand the active tectonics of western Kosovo and make implications on its seismicity, we obtained results from different geomorphometric analyses, geomorphological observations, and structural measurements.

According to the results of geomorphometric analyses of the studied four different mountain fronts, the Pejë, Istog, Krojmir, and Prizren faults are all classified in Class I as high activity and indicating tectonic uplift rates of over 0.5 mm/a according to the calculated S_{mf} and V_f values. Among them, the ENE-WSW trending Istog fault clearly separated from the others with its higher B_s and *HI* values indicating its higher activity. The NNW-SSE-directed Krojmir, the NNE-SSW trending Pejë, and the NE-SW-oriented Prizren faults follow it, respectively. However, all the studied faults are highly active and can create earthquakes with magnitudes between 6.4 and 6.8, if they will be ruptured all along the related mountain fronts. On the other hand, according to k_{sn} values, the Pejë and Istog faults are clearly the highest and indicate a probable structural continuity. As known for a long time, the orogens of Dinarides to the north and Albanides-Hellenides to the south are separated by a fault zone known as the Shkodër-Pejë fault zone reaching northern Kosovo. According to the geomorphometric analyses, the Istog fault can be interpreted as the eastern continuity of the Shkodër-Pejë fault zone together with the Pejë fault and represent its importance for the seismicity of western Kosovo. In the field, we observed many indicators of high activity/rapid uplift along the studied mountain front faults imprinted geomorphologically, such as trapezoidal to triangular facets, steep scarps, deeply incised valleys, and well-developed alluvial fan deposits. On the other hand, according to the collected kinematic data from the fault planes observed on each of the studied faults, the NNE-SSW trending Pejë, the ENE-WSW-directed Istog, and the NE-SW-oriented Prizren faults are normal faults, and represent NW-SE-directed extension. The NW-SE trending Krojmir fault represents an oblique and normal character with NE-SW-oriented extension.

Relative activity and general structural pattern of the studied faults indicate the dominant role of the eastern part of the Shkodër-Pejë fault zone in western Kosovo (i.e., Pejë and Istog faults) and the major role of NW-SE-directed active extension. This extension is most probably caused by the effect of the rollback of the subducting slab in the Hellenic trench and the related clockwise rotation of the Albanides-Hellenides to the south of the Shkodër-Pejë fault zone. However, for a well-understanding of the active tectonics and seismicity of whole the country, eastern Kosovo should also be studied, where the structural pattern seems a little bit different and the major part of the population and industry of the country is hosted.

Acknowledgements

The authors are grateful to two reviewers for their constructive criticisms and to Dr. Ercan SANGU for suggestions on the kinematic analysis. The stress analysis results were obtained using Win-Tensor, a software developed by Dr. Damien DELVAUX, Royal Museum for Central Africa, Tervuren, Belgium.

References

Aliaj, Sh. 1988. Neotectonics and seismicity of Albania. Ph.D. Thesis, 265, Archive of Seismological Institute, Albanian.

Aubouin, J., Blanchet, R., Cadet, J. P., Celet, P., Charvet, J., Chorowicz, J., Cousin, M., Rampnoux, J. P. 1970. Essai sur la géologie des Dinarides. Bulletin de la Société géologique de France 7(6), 1060-1095.

Baker, C., Hatzfeld, D.L., Lyon-Caen, H., Papadimitriou, E., Rigo, A. 1997. Earthquake mechanisms of the Adriatic Sea and Western Greece: Implications for the oceanic subduction-continental collision transition. Geophysical Journal International 131(3), 556-594.

Benetatos, C., Kiratzi, A. 2006. Finite-fault slip models for the 15 April 1979 (Mw 7.1) Montenegro earthquake and its strongest aftershock of 24 May 1979 (Mw 6.2). Tectonophysics 421 (1–2), 129–143.

Biermanns, P., Schmitz, B., Ustaszewski, K., Reicherter, K. 2019. Tectonic geomorphology and Quaternary landscape development in the Albania – Montenegro border region: an inventory. Geomorphology 326, 116–131.

Biermanns, P., Schmitz, B., Mechernich, S., Weismüller, C., Onuzi, K., Ustaszewski, K., Reicherter, K. 2022. Aegean-style extensional deformation in the contractional southern Dinarides: incipient normal fault scarps in Montenegro. Solid Earth 13(6), 957-974.

Bradley, K. E., Vassilakis, E., Hosa, A., Weiss, B. P. 2013. Segmentation of the Hel-lenides recorded by Pliocene initiation of clockwise block rotation in Central Greece. Earth Planet Science Letters 362, 6–19.

Bull, W. B., McFadden, L. D. 1977. Tectonic geomorphology north and south of the Garlock Fault, California. Doehering, D. O. (Ed.). Geomorphology of Arid Regions. Binghamton, State University of New York, Proceedings of the 8th Annual Geomorphology Symposium Proceedings, 115-138.

Burchfiel, C. B., Nakov, R., Tzankov, T., Royden, L. H. 2000. Cenozoic extension in Bulgaria and northern Greece: the northern part of the Aegean extensional regime. Geological Society of London, Special Publications 173(1), 325-352.

Burchfiel, B. C., King, R. W., Todosov, A., Kotzev, V., Durmurdzanov, N., Serafimovski, T., Nurce, B. 2006. GPS results for Macedonia and its importance for the tectonics of the Southern Balkan extensional regime. Tectonophysics 413(3-4), 239-248.

Burchfiel, B. C., King, R. W., Nakov, R., Tzankov, T., Dumurdzanov, N., Todosov, A., Nurce, B. 2008. Patterns of Cenozoic Extensional Tectonism in the South Balkan Extensional System. In Earthquake Monitoring and Seismic Hazard Mitigation in Balkan Countries, Springer, Dordrecht.

Cheng, Y., He, C., Rao, G., Yan, B., Lin, A., Hu, J., Yangli, L., Yao, Q. 2018. Geomorphological and structural characterization of the southern Weihe Graben, central China: Implications for fault segmentation. Tectonophysics 722, 11-24.

Chiba, T., Kaneta, S. I., Suzuki, Y. 2008. Red relief image map: new visualization method for three dimensional data. The International Archives of the Photogrammetry, Remote Sensing and Spatial Information Sciences 37(B2), 1071-1076.

D'Agostino, N., Avallone, A., Cheloni, D., D'Anastasio, E., Mantenuto, S., Selvaggi, G. 2008. Active tectonics of the Adriatic region from GPS and earthquake slip vectors. Journal of Geophysical Research 113(B12), B0940.

D'Agostino, N., Métois, M., Koci, R., Duni, L., Kuka, N., Ganas, A., Georgiev, I., Jouanne, F., Kaludjerovic, N., Kandić, R. 2020. Active crustal deformation and rotations in the southwestern Balkans from continuous GPS measurements. Earth and Planetary Science Letters *539*, 116246.

D'Agostino, N., Copley, A., Jackson, J., Koçi, R., Hajrullai, A., Duni, L., Kuka, N. 2022. Active tectonics and fault evolution in the Western Balkans. Geophysical Journal International 231(3), 2102-2126.

Delvaux, D., Sperner, B. 2003. Stress tensor inversion from fault kinematic indicators and focal mechanism data: the TENSOR program. Nieuwland, D. (Ed.). New Insights into Structural Interpretation and Modelling. Geological Society of London, Special Publications 212, 75-100.

Dibiase, R. A., Whipple, K. X., Heimsath, A. M., Ouimet, W. B. 2010. Landscape form and millennial erosion rates in the San Gabriel Mountains, CA. Earth and Planetary Science Letters 289(1-2), 134-144.

Dumurdzanov, N., Serafimovski, T., Burchfiel, B. C. 2005. Cenozoic tectonics of Macedonia and its relation to the South Balkan extensional regime. Geosphere 1(1), 1-22.

Elezaj, Z. 2002. Seismotectonic characteristics of Kosovo as basis for its seismic zonation. Ph.D. Thesis, Prishtina, Kosovo (in Albanian).

Elezaj, Z. 2009. Seismotectonic settings of Kosovo. Journal of International Environmental Application and Science 4(2), 167-176.

Elezaj, Z. 2012. Late and young tectonics (Neotectonics) and seismicity of Kosovo. Journal of International Environmental Application and Science 7(4), 744-749.

Elezaj, Z., Kodra, A. 2007. Gjeologjia e Kosovës. Univ. i Prishtinës, Fak. i Xehetarisë dhe Metalurgjisë Mitrovicë 293.

El Hamdouni, R., Irigaray, C., Fernández, T., Chacón, J., Keller, E. A. 2008. Assessment of relative active tectonics, southwest border of the Sierra Nevada (southern Spain). Geomorphology 96(1-2), 150-173.

Faccenna, C., Jolivet, L., Piromallo, C., Morelli, A. 2003. Subduction and the depth of convection in the Mediterranean mantle. Journal of Geophysical Research: Solid Earth 108(B2), 2099.

Facenna, C., Becker, T.W., Auer, L., Billi, A., Boschi, L., Brun, J.P., Capitanio, F.A., Funiciello, F., Horvàth, F., Jolivet, L., Piromallo, C., Royden, L., Rossetti, F., Serpelloni, E. 2014. Mantle dynamics in the Mediterranean. Review of Geophysics 52(3), 283-332.

Flint, J. J. 1974. Stream gradient as a function of order, magnitude, and discharge. Water Resources Research, 10(5), 969-973.

Han, Z., Li, X., Wang, N., Chen, G., Wang, X., Lu, H. 2017. Application of river longitudinal profile morphometrics to reveal the uplift of Lushan Mountain. Acta Geologica Sinica 91(5), 1644–1652.

Handy, M. R., Ustaszewski, K., Kissling, E. 2015. Reconstructing the Alps–Carpathians–Dinarides as a key to understanding switches in subduction polarity, slab gaps and surface motion. International Journal of Earth Sciences 104(1), 1-26.

Handy, M. R., Giese, J., Schmid, S. M., Pleuger, J., Spakman, W., Onuzi, K., Ustaszewski, K. 2019. Coupled crust-mantle response to slab tearing, bending, and rollback along the Dinaride-Hellenide orogen. Tectonics 38(8), 2803-2828.

Hare, P. W., Gardner, T. W. 1985. Geomorphic indicators of vertical neotectonism along converging plate margins, Nicoya Peninsula, Costa Rica. Tectonic Geomorphology 4, 75-104.

Harlin, J. M. 1978. Statistical moments of the hypsometric curve and its density function. Journal of the International Association for Mathematical Geology 10(1), 59-72.

Hollenstein, C., Müller, M.D., Geiger, A., Kahle, H. G. 2008. Crustal motion and deformation in Greece from a decade of GPS measurements, 1993–2003. Tectonophysics 449(1-4), 17-40.

Jouanne, F., Mugnier, J. L., Koçi. R., Bushati., S., Matev, K., Kuka, N., Shinko, I., Koçiaj, S., Duni, L. 2012. GPS constrains on current tectonics of Albania. Tectonophysics 554-557, 50-62.

Keller, E. A. 1986. Investigation of active tectonics: use of surficial Earth processes, In Wallace (Ed.). Active Tectonics, Studies in Geophysics, National Academy Press, Washington, DC, 136–147.

Keller, E. A., Pinter N. 2002. Active Tectonics: Earthquakes, Uplift and Landscapes. Prentice Hall, New Jersey.

Kirby, E., Whipple, K. X. 2012. Expression of active tectonics in erosional landscapes. Journal of Structural Geology 44, 54–75.

Kissel, C., Laj, C. 1988. The tertiary geodynamical evolution of the Aegean arc: a paleomagnetic reconstruction. Tectonophysics 146, 183–201.

Kissel, C., Speranza, F., Milicevic, V. 1995. Paleomagnetism of external southern and central Dinarides and northern Albanides: implications for the Cenozoic activity of the Scutari-Pec transverse zone. Journal of Geophysical Research, Solid Earth (1978–2012)100 (100), 14999–15007.

Kothyari, G. C., Kotlia, B. S., Talukdar, R., Pant, C .C., Joshi, M. 2020. Evidences of neotectonic activity along Goriganga river, higher central Kumaun Himalaya, India. Geological Journal 55(9), 6123-6146.

Kotzev, K., Nakov, R., Georgiev, T., Burchfiel, B., King, R. 2006. Crustal motion and strain accumulation in western Bulgaria. Tectonophysics 413, 127–145.

KPMM. 2006. Geological map of Kosovo 1:200,000 scale. Komisioni i Pavarur për Miniera dhe Minerale, Prishtinë, Kosovo, 1 sheet.

Le Pichon, X., Kreemer, C. 2010. The Miocene-to-present kinematic evolution of the Eastern Mediterranean and Middle East and its implications for dynamics. Annual Review of Earth and Planetary Sciences 38, 323–351.

Louvari, E., Kiratzi, A., Papazachos, B., Hatzidimitriou, P. 2001. Fault-plane solutions determined by waveform modeling confirm tectonic collision in the Eastern Adriatic. Pure Applied Geophysics 158, 1613–1637.

Mayer, L. 1990. Introduction to Quantitative Geomorphology. Prentice Hall, Englewood, Cliffs, NJ.

McClusky, S., Balassanian, S., Barka, A., Demir, C., Ergintav, S., Georgiev, I., Gurkan, O., Hamburger, M., Hurst, K., Kahle, H., Kastens, K., Kekelidze, G., King, R., Kotzev, V., Lenk, O., Mahmoud, S., Mishin, A., Nadariya, M., Ouzounis, A., Paradissis, D., Peter, Y., Prilepin, M., Reilinger, R., Sanli, I., Seeger, H., Tealeb, A., Toksöz,

M.N., Veis, G. 2000. Global positioning system constraints on plate kinematics and dynamics in the eastern Mediterranean and Caucasus. Journal of Geophysical Research and Solid Earth 105, 5695–5719.

Métois, M., D'Agostino, N., Avallone, A., Chamot-Rooke, N., Rabaute, A., Duni, L., Kuka, N., Koci, R., Georgiev, I. 2015. Insights on continental collisional processes from GPS data: dynamics of the peri-Adriatic belts. Journal of Geophysical Research and Solid Earth 120, 8701–8719.

Muço, B. 1998. Catalogue of ML 3,0 earthquakes in Albania from 1976 to 1995 and distribution of 25 seismic energy released. Tectonophysics 292, 311–319.

Muço, B., Alexiev, G., Aliaj, S., Elezi, Z., Grecu, B., Mandrescu, N., Milutinovic, Z., Radulian, M., Ranguelov, B., Shkupi, D. 2012. Geohazards assessment and mapping of some Balkan countries. Natural Hazards 64(2), 943-981.

Mustafa, S. 2016. Characteristic of the tectonic, seismicity, active faults and earth crust model, as basis for generation of synthetic accelerograms. PhD Thesis, "Ss. Cyril and Methodius" University in Skopje, Institute of Earthquake Engineering and Engineering Seismology – Skopje Republic of Macedonia, 193 p.

Mustafa, S., Krelani, V., Beqiri, L., Sinani, B. 2020. Seismic activity and essential seismological characteristics of the Kosovo territory. UBT International Conference 242.

Nocquet, J. M. 2012. Present-day kinematics of the Mediterranean: a comprehensive overview of GPS results. Tectonophysics 579, 220–242.

Orana, Xh., Arsovski, M., Mihailov, V. 1985. The seismotectonic features of Kosovo. IZIIS, Skopje (in Macedonian).

Papa, A., Hyseni, A., Leci, V., Prence J. 1991. Pasqyrini istilit tektonik të Albanideve të Jashtne në molasën er.rltësirës pranadtrietike. Bu.l. Sbken. Gjeol. 1, 197-206.

Papadopoulos, G. A., Agalos, A., Carydis, P., Lekkas, E., Mavroulis, S., Triantafyllou, I. 2020. The 26 November 2019 Mw 6.4 Albania Destructive Earthquake. Seismological Society of America 91(6), 3129-3138.

Pike, R. J., Wilson, S. E. 1971. Elevation–relief ratio, hypsometric integral, and geomorphic area-altitude analysis. Geological Society of America Bulletin 82, 1079–1084.

Ramírez-Herrera, M. T. 1998. Geomorphic assessment of active tectonics in the Acambay Graben, Mexican volcanic belt. Earth Surface Processes and Landforms 23(4), 317-332.

Reilinger, R .E., McClusky, S. C., Oral, M. B., King, R. W., Toksöz, M .N. 1997. Global positioning system measurements of present-day crustal movements in the Arabia–Africa–Eurasia plate collision zone. Journal of Geophysical Research 102, 9983–9999.

Reilinger, R, McClusky, S., Vernant, P., Lawrence, S., Ergintav, S., Cakmak, R., Özener, H., Kadirov, F.,Guliev, İ., Stepanyan, R., Nadariya, Hahubia, G., Mahmoud, S K. Sakr, ArRajehi, A., Paradissis,D., A. Al-Aydrus, A., Prilepin, M., Guseva, T., Evren, E., Dmitrotsa, A., Filikov, S. V., Gomez, F., Al-Ghazzi,R., Karam, G. 2006. GPS constraints on continental deformation in the Africa-Arabia-Eurasia continental collision zone and implications for the dynamics of plate interactions. Journal of Geophysical Research 111, B05411.

Rockwell, T. K., Keller, E. A., Johnson, D. L. 1985. Tectonic geomorphology of alluvial fans and mountain fronts near Ventura, California. In: Morisawa, M. (Ed.). Tectonic Geomorphology. Proceedings of the 15th Annual Geomorphology Symposium. Allen and Unwin Publishers, Boston, MA, 183–207.

Schmid, S. M., Fügenschuh, B., Kounov, A., Maţenco, L., Nievergelt, P., Oberhänsli, R., ... van Hinsbergen, D. J. 2020. Tectonic units of the Alpine collision zone between Eastern Alps and western Turkey. Gondwana Research 78, 308-374.

Schmitz, B., Biermanns, P., Hinsch, R., Đaković, M., Onuzi, K., Reicherter, K., Ustaszewski, K. 2020. Ongoing shortening in the Dinarides fold-and-thrust belt: A new structural model of the 1979 (Mw 7.1) Montenegro earthquake epicentral region. Journal of Structural Geology 141, 104192.

Silva, P. G., Goy, J. L., Zazo, C., Bardajı, T. 2003. Fault-generated mountain fronts in southeast Spain: geomorphologic assessment of tectonic and seismic activity. Geomorphology 50(1-3), 203-225.

Snyder, N. P., Whipple, K. X., Tucker, G. E., Merritts, D. J. 2000. Landscape response to tectonic forcing: DEM analysis of stream profiles in the Mendocino triple junction region, northern California. Geological Society of America Bulletin 112(8), 1250 – 1263.

Speranza, F., Islami, I., Kissel, C., Hyseni, A. 1995. Paleomagnetic evidence for Ceno-zoic clockwise rotation of the external Albanides. Earth Planet of Science Letters 129, 121–134.

Strahler, A. N. 1952. Hypsometric (area-altitude) analysis of erosional topography. The Geological Society of America Bulletin 63(11), 1117-1142.

Sulstarova, E., Aliaj Sh. 2001. Seismic hazard assessment in Albania. In: Muço, B., Fuga, P. (Ed.). Albanian Journal of Natural and Technical Sciences X, 89–101.

Sukhishvili, L., Forte, A. M., Merebashvili, G., Leonard, J., Whipple, K. X., Javakhishvili, Z., Heimsath, A., Godoladze, T. 2021. Active deformation and Plio-Pleistocene fluvial reorganization of the western Kura fold–thrust belt, Georgia: implications for the evolution of the Greater Caucasus Mountains. Geological Magazine 158(4), 583-597.

Sun, L., Mann, P. 2021. Along-Strike Rapid Structural and Geomorphic Transition From Transpression to Strike-Slip to Transtension Related to Active Microplate Rotation, Papua New Guinea. Frontiers in Earth Scienc, 9, 652352.

Taymaz, T., Jackson, J., Westaway, R. 1990. Earthquake mechanisms in the Hellenic Trench near Crete. Geophysical Journal of International 102, 695–731.

Ulusoy, İ., Diker, C., Şen, E., Aydın, E., Akkaş, E., Gümüş, E., ... Erkut, V., 2020. Surface expressions of morphostructural features at Hasandağ stratovolcano on DEM datasets. Mediterranean Geoscience Reviews, 1-17.

Wells, D. L., Coppersmith, K. J. 1994. New empirical relationships among magnitude, rupture length, rupture width, rupture area, and surface displacement. Bulletin of the Seismological Society of America 84(4), 974-1002.

Whipple, K. X. 2004. Bedrock rivers and the geomorphology of active orogens. Annual Revision Earth Planet of Science, 32, 151-185.

Wobus, C., Whipple, K. X., Kirby, E., Snyder, N., Johnson, J., Spyropolou, K., Crosby, B., Sheehan, D. 2006. Tectonics from topography: Procedures, promise, and pitfalls. In: Willett, S. D., Hovius, N., Brandon, M. T., Fisher, D. M.(Ed.). Tectonics, Climate, and Landscape Evolution, 55–74. Geological Society of America.

van Hinsbergen, D., Langereis, C., Meulenkamp, J. 2005. Revision of the timing magnitude and distribution of Neogene rotations in the western Aegean region. Tectonophysics 396, 1–34.

Yao, W., Liu-Zeng, J., Oskin, M. E., Wang, W., Li, Z., Prush, V., ... Klinger, Y. 2019. Reevaluation of the late Pleistocene slip rate of the Haiyuan fault near Songshan, Gansu Province, China. Journal of Geophysical Research: Solid Earth 124(5), 5217-5240.

Yokoyama, R., Shirasawa, M., Pike, R. J. 2002. Visualizing topography by openness: a new application of image processing to digital elevation models. Photogrammetric Engineering and Remote Sensing 68(3), 257-266.